On the Trade-off Between Accuracy and Delay in UWB Navigation

Gabriel E. Garcia, L. Srikar Muppirisetty, and Henk Wymeersch, *Member, IEEE*

***Abstract*—We investigate the relation between medium access control (MAC) delay and ultra-wide bandwidth (UWB) tracking accuracy. We quantify this relation by deriving fundamental lower bounds on tracking accuracy and MAC delay for arbitrary finite networks. Our main finding is that the traditional ways to increase accuracy (e.g., increasing the number of anchors or the transmission power) may lead to large MAC delays. We evaluate two methods to mitigate these delays.**

***Index Terms*—Ultra-wideband, S-TDMA, MAC delay, navigation, positioning**

I. Introduction

LOCATION-aware technologies are evolving in a fast-paced manner, enabling numerous applications in the public, commercial, and military sectors. The need for accurate navigation in GPS-challenged scenarios can be addressed by ultra-wide bandwidth (UWB) ranging and communication [1]. Our focus is on ranging using two-way time-of-arrival (TW-TOA) estimation.

A large body of work has been devoted to develop ways to improve positioning accuracy: improved ranging algorithms, increased bandwidth and/or transmission power [2], and the use of cooperation among nodes [3]. The general conclusion is that performance is improved by using more anchors, higher transmission powers, and cooperation. Based on navigation experiments with off-the-shelf UWB radios [4], we found that in practice, these performance gains come at a cost in delay, due to the channel accesses required. Constrained by dynamics of the agents and the IEEE 802.15.4a standard, the impact of medium access control (MAC) has been studied in [5]–[8]: [5] proposes enhancements to the 802.15.4a standard using a time division multiple access (TDMA) approach for clique networks. In [6], the authors present further enhancements to [5] to reduce MAC delay, but do not consider the impact on positioning accuracy. Through simulation, [7] evaluates different TDMA-based prioritization strategies. Finally, [8] considers an IEEE 802.11.b MAC and investigates the interaction between MAC delay and positioning accuracy. However, this MAC is inefficient in terms of throughput and thus gives overly pessimistic delay estimates.

In this paper, we derive lower bounds on UWB positioning accuracy and required MAC delay to perform two-way ranging, enabling an understanding of their trade-off and allowing designers a fast way to dimension UWB navigation networks. We find that large delays are incurred when the number of anchors or the transmission power are increased indiscriminately. We evaluate two methods to reduce the delay: selective ranging [7] and eavesdropping [9].

The authors are with the Communication Systems Group, Department of Signals and Systems, Chalmers University of Technology, SE-412 96 Gothenburg, Sweden. Email: {ggarcia,srikar.muppirisetty,henkw}@chalmers.se.

This research was supported in part, by the European Research Council, under Grant No. 258418 (COOPNET), and the Swedish Research Council, under Grant No. 2010-5889.

II. System Model

A. UWB Navigation

We consider a wireless network consisting of N mobile agent nodes (collected in the set $\mathcal{S}_{\text{agents}}$) and M anchors nodes (collected in the set $\mathcal{S}_{\text{anchors}}$). Agents move in discrete time slots of duration T. The position of node i at time slot t is denoted by $\mathbf{x}_i^{(t)}$, while the TW-TOA measurements made by agent i at time slot t are denoted by $\mathbf{z}_i^{(t)}$. We assume the following discrete-time model for the agents [10]:

$$\mathbf{x}_i^{(t)} = f_{\text{state}}(\mathbf{x}_i^{(t-1)}) + \mathbf{v}_i^{(t)} \quad (1)$$

$$\mathbf{z}_i^{(t)} = f_{\text{meas}}(\mathbf{x}_i^{(t)}) + \mathbf{w}_i^{(t)}, \quad (2)$$

where the noise terms $\mathbf{v}_i^{(t)}$ and $\mathbf{w}_i^{(t)}$ capture randomness in mobility and ranging errors, respectively. Agent i tracks its own position by recursively predicting an a priori distribution, $p(\mathbf{x}_i^{(t)}|\mathbf{z}_i^{(1:t-1)})$, and then correcting to an a posteriori distribution $p(\mathbf{x}_i^{(t)}|\mathbf{z}_i^{(1:t)})$, before moving on to the next time slot. Clearly, shorter slots are required to support faster mobility.

The time slot duration T can thus be broken up into a measurement time T_{meas} and a computation time T_{comp}. Assuming that the measurement time is dominant, we aim to quantify how adding more anchors or increasing the communication range affects the accuracy (determined by the position error bound [2]) and T_{meas} (determined by the MAC delay), and in turn the minimal required T. We focus on a single time slot, and thus assume a known a priori distribution $p(\mathbf{x}_i^{(t)}|\mathbf{z}_i^{(1:t-1)})$. For notational convenience, the superscript t will be dropped.

B. Network Model

Following [11], nodes i and j can communicate with probability $P_{ij} = \exp\left(- \parallel \mathbf{x}_i - \mathbf{x}_j \parallel^2 / (2R^2)\right)$, where R is the nominal communication range in meters. Once links are realized, we define the communication graph $G = (V, E)$ comprising a set V of nodes and a set E of communication links. We further introduce $\mathbf{A}$, the symmetric adjacency matrix of G, and $\mathbf{S}$, the scheduling matrix, with $S_{ij} = 1$ if the link (i, j) is to be scheduled for TW-TOA, and $S_{ij} = 0$ otherwise. Note that $S_{ij} = 1 \Rightarrow A_{ij} = 1$. From $\mathbf{A}$, we can also introduce the neighborhood of a node i, $\mathcal{N}_i = \{j \neq i : A_{ij} = 1\}$.

Two TW-TOA transactions can only be active simultaneously if they do not interfere. As 802.15.4a radios use a common preamble, similar to our off-the-shelf-radios, we cannot rely solely on time-hopping to deal with interference, and traditional protocols such as ALOHA or slotted ALOHA [12] have poor efficiency in terms of the successful number of transactions. Hence, similar to [5]–[7], we consider a TDMA MAC with spatial reuse (S-TDMA), where each TW-TOA transaction requires one time slot. This implies that when any of the four radios involved in two TW-TOA transactions are adjacent (according to $\mathbf{A}$), then the two transactions must be scheduled in distinct TDMA slots. In contrast to [6], we do not consider ranging packet aggregation or other enhancements, as they are hard to justify with real hardware, mainly because of the tight synchronization requirements.

C. Measurement Models

We consider two types of measurements: TW-TOA and eavesdropping. In TW-TOA, agent i sends a request to anchor j, which estimates the TOA and responds back with an acknowledgment. Agent i measures the time of the TOA. The TW-TOA measurement between agent i and anchor j is given by [9]:

$$z_{ij} = \underbrace{d_{ij} + \frac{cT_{\mathrm{proc}}}{2}}_{=\mu_{ij}} + \frac{n_{ij}}{2} + \frac{n_{ji}}{2}, \tag{3}$$

where c is the speed of light, T_{proc} is a known processing time, $d_{ij} = \| \mathbf{x}_i - \mathbf{x}_j \|$, n_{ij} is the TOA error of the request from node i to node j and n_{ji} is the TOA error from the acknowledgement from node j to node i. The errors are modeled as independent zero-mean Gaussian random variables: $n_{ij} \sim \mathcal{N}(0, \sigma_{ij}^2)$ and $n_{ji} \sim \mathcal{N}(0, \sigma_{ji}^2)$. In eavesdropping, we allow any node $k \in \mathcal{N}_i \cap \mathcal{N}_j$ to measure the TOA of the signals exchanged between nodes i and j. Subtracting those two TOA measurements, we obtain an eavesdropping measurement [9]:

$$z_{ij}^k = \underbrace{d_{ij} + d_{jk} - d_{ik} + cT_{\mathrm{proc}}}_{=\mu_{ij}^k} + n_{ij} + n_{jk} - n_{ik}. \tag{4}$$

Note that there is a common noise term between (3) and (4), since one of the TOA measurements collected by node k depends on the TOA measurement of node j.

III. Lower Bound on Positioning Accuracy

In this section, we will compute the position error bound (PEB) [2] for a network with TW-TOA and eavesdropping measurements. We collect the positions of all the agents in a vector $\mathbf{p} = \left[\mathbf{x}_1^{\mathrm{T}} \mathbf{x}_2^{\mathrm{T}} \cdots \mathbf{x}_N^{\mathrm{T}}\right]^{\mathrm{T}}$. For mathematical convenience, we further assume that every agent's position has an a priori distribution $p(\mathbf{x}_i^{(t)} | \mathbf{z}_i^{(1:t-1)})$, which is a symmetric Gaussian distribution with mean $\mathbf{m}_{\mathrm{prior},i}$ and variance $\sigma_{\mathrm{prior},i}^2$ per dimension. Let us further construct a measurement vector $\mathbf{z}$ as

$$\mathbf{z} = \left\{ \mathbf{z}_{ij} | i \in \mathcal{S}_{\mathrm{agents}},\, j \in \mathcal{N}_i \cap \mathcal{S}_{\mathrm{anchors}} \right\}, \tag{5}$$

in which $\mathbf{z}_{ij}$ contains the TW-TOA estimate between agent i and anchor j, as well as all corresponding eavesdropping measurements:

$$\mathbf{z}_{ij} = \left[z_{ij},\, \left\{ z_{ij}^k \middle| k \in \mathcal{N}_i \cap \mathcal{N}_j \right\} \right].$$

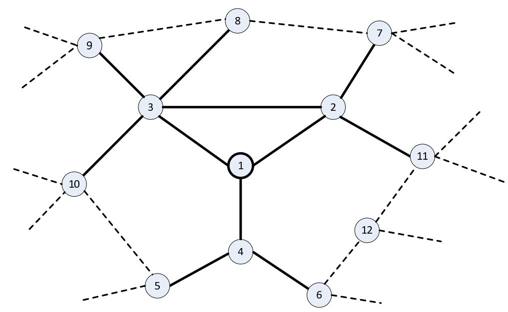

Figure 1. Subnetwork associated with node 1 within the larger network topology.

Due to (3) and (4), $\mathbf{z}$ conditioned on $\mathbf{p}$ is a Gaussian random variable with mean $\boldsymbol{\mu}$, constructed from (3) and (4) in the same way as $\mathbf{z}$, and covariance matrix $\boldsymbol{\Sigma}$, structured as detailed in the Appendix.

The PEB is defined as $\mathcal{P} = \sqrt{\mathrm{tr}\left\{\mathbf{J}^{-1}\right\}/N}$, where $\mathbf{J}$ is the Bayesian Fisher information matrix [2]:

$$\begin{aligned}
\mathbf{J} &= -\mathbb{E}_{\mathbf{p},\mathbf{z}} \left\{ \nabla_{\mathbf{p}} \nabla_{\mathbf{p}}^{\mathrm{T}} \log p(\mathbf{z}, \mathbf{p}) \right\} && (6)\\
&= -\mathbb{E}_{\mathbf{p},\mathbf{z}} \left\{ \nabla_{\mathbf{p}} \nabla_{\mathbf{p}}^{\mathrm{T}} \log p(\mathbf{z}|\mathbf{p}) \right\} - \mathbb{E}_{\mathbf{p}} \left\{ \nabla_{\mathbf{p}} \nabla_{\mathbf{p}}^{\mathrm{T}} \log p(\mathbf{p}) \right\} \\
&= -\mathbb{E}_{\mathbf{p}} \left\{ \nabla_{\mathbf{p}} \boldsymbol{\mu}^{\mathrm{T}} \boldsymbol{\Sigma}^{-1} \nabla_{\mathbf{p}}^{\mathrm{T}} \boldsymbol{\mu} \right\} + \mathbf{J}_{\mathrm{prior}}. && (7)
\end{aligned}$$

where $\nabla_{\mathbf{p}}$ denotes the derivative with respect to $\mathbf{p}$ and where $\mathbf{J}_{\mathrm{prior}} = \mathrm{diag}\left[\sigma_{\mathrm{prior},1}^2, \sigma_{\mathrm{prior},1}^2, \ldots, \sigma_{\mathrm{prior},N}^2, \sigma_{\mathrm{prior},N}^2\right]^{-1}$. The entries in the matrix $\nabla_{\mathbf{p}} \boldsymbol{\mu}^{\mathrm{T}}$, can be easily computed since

$$\begin{aligned}
\frac{\partial \mu_{ij}}{\partial \mathbf{x}_i} &= \frac{\mathbf{x}_i - \mathbf{x}_j}{d_{ij}} \\
\frac{\partial \mu_{ij}^k}{\partial \mathbf{x}_i} &= \frac{\mathbf{x}_i - \mathbf{x}_j}{d_{ij}} - \frac{\mathbf{x}_i - \mathbf{x}_k}{d_{ik}} \\
\frac{\partial \mu_{ij}^k}{\partial \mathbf{x}_k} &= \frac{\mathbf{x}_k - \mathbf{x}_j}{d_{kj}} - \frac{\mathbf{x}_k - \mathbf{x}_i}{d_{ik}}.
\end{aligned}$$

The expectation over $\mathbf{p}$ in (7) can be performed through Monte Carlo integration. Note that evaluation of the PEB is computationally easy, since $\boldsymbol{\Sigma}$ is block-diagonal and $\nabla_{\mathbf{p}} \boldsymbol{\mu}^{\mathrm{T}}$ is sparse.

IV. Bounds on Minimum MAC Delay

The problem of assigning TDMA slots to avoid interference is known as strong edge coloring, which is an NP-complete problem. This complexity issue can be avoided by considering special networks [6] or resorting to computer simulations [5], [7], [8]. Here, in contrast, we seek lower (Υ) and upper (Ω) bounds on the total number of TDMA time slots to schedule the links from $\mathbf{S}$, given the adjacency matrix $\mathbf{A}$.

Upper bounds: A trivial upper bound is the number of links to be scheduled, $\Omega_1 = (\mathbf{1}^T \mathbf{S} \mathbf{1})/2$, where $\mathbf{1}$ is a vector of ones. A second upper bound was conjectured by Erdős-Nešetřil [13] and is given by $\Omega_2 = \frac{5}{4}\Delta^2$ for even Δ and $\Omega_2 = \frac{1}{4}(5\Delta^2 - 2\Delta + 1)$ for odd Δ, where Δ is the maximum $\mathbf{S}$-degree.[1] Hence, our final upper bound is $\Omega = \min(\Omega_1, \Omega_2)$.

Algorithm 1 Lower bound on number of TDMA time slots.

Input: Adjacency matrix $\mathbf{A}$ and scheduling matrix $\mathbf{S}$
for $i = 1$ to $N + M$ **do**
  $\mathbf{q}_i = \texttt{find}(\mathbf{a}_i)$;
  for $j \in \mathbf{q}_i$ **do**
    $\mathbf{b}_{ij} = \mathbf{a}_i \otimes \mathbf{a}_j + \mathbf{e}_j$;
    $\mathbf{g}_{ij} = \texttt{find}(\mathbf{b}_{ij})$;
    $T_{ij} = \Delta_i + \mathbf{b}_{ij}^T(\boldsymbol{\Delta} - \mathbf{1} + \mathbf{a}_i \oplus \mathbf{s}_i) - (\mathbf{1}^T\, \mathbf{S}[\mathbf{g}_{ij}, \mathbf{g}_{ij}]\, \mathbf{1})/2$;
  end for
end for
$\Upsilon_2 = \max_{i,j} T_{ij}$;

Lower bounds: A trivial, but very loose lower bound is $\Upsilon_1 = \Delta$, since every link in $\mathbf{S}$ related to one node must be scheduled in a distinct TDMA slot. We also present a constructive lower bound, by considering simple subnetworks of the original network and finding a lower bound on the number of TDMA time slots for that subnetwork. The maximum of the lower bounds over these subnetworks gives a global lower bound, $\Upsilon_2 \geq \Upsilon_1$. Note that for clique networks, $\Upsilon_2 = \Omega$.

The constructive lower bound is found as follows (see Fig. 1, for a simple example with $\mathbf{A} = \mathbf{S}$): consider a node i, one of its neighbors j, as well as any common neighbors, $\mathcal{N}_i \cap \mathcal{N}_j$. For $(i, j) = (1, 4)$, to schedule the links for both nodes we need $\Delta_1 + \Delta_4 - 1 = 5$ TDMA time slots. Similarly, for $(i, j) = (1, 2)$, $\mathcal{N}_1 \cap \mathcal{N}_2 = 3$, we need $\Delta_1 + (\Delta_2 - 1 + \Delta_3 - 1) - 1 = 9$ TDMA time slots. In both examples, the last term accounts for any common edges that would be assigned two slots. An algorithm that formalizes this reasoning is given in Algorithm 1, with the following notations: $\mathbf{a}_i$ and $\mathbf{s}_i$ are the i-th column of the adjacency and scheduling matrix, respectively; $\mathbf{e}_j$ is a vector of all zeros except for a 1 at the j-th location; Δ_i is the $\mathbf{S}$-degree of node i and $\boldsymbol{\Delta} = [\Delta_1, \Delta_2, \ldots, \Delta_{N+M}]^{\mathrm{T}}$; $\oplus$ is the binary field sum; $\otimes$ is the binary field product; the `find` operator returns the indices to non-zero elements of the argument.

V. Results and Discussion

A. Simulation Setup

Nodes are placed inside a 20 m $\times$ 20 m square: agents are uniformly distributed in the area, while anchors are placed according to a scaled network topology from [3, Fig. 13]. Based on our experimental results with the P400 UWB radios [4], we consider a ranging standard deviation of 2 cm (irrespective of distance under line-of-sight propagation) and TDMA time slot duration of 20 ms. The a priori distributions of the agents' positions are Gaussian with unity variance.

We will evaluate the PEB and the upper and lower bound on the MAC delay, for the following scenarios: (i) TW-TOA with all anchors in communication range; (ii) TW-TOA with all anchors in communication range plus eavesdropping; (iii) TW-TOA with at most[2] 4 anchors; (iv) TW-TOA with at most 4 anchors plus eavesdropping. For each scenario, we will evaluate the impact of the number of anchors and the communication range. Note that the MAC delay values are not affected by eavesdropping, so MAC delay curves for scenarios (i) and (ii) will be the same, as will those for scenarios (iii) and (iv).

[1]The $\mathbf{S}$-degree of node i is the sum of the entries of the i-th row in $\mathbf{S}$.

[2]Selected using a simple greedy algorithm to minimize the PEB.

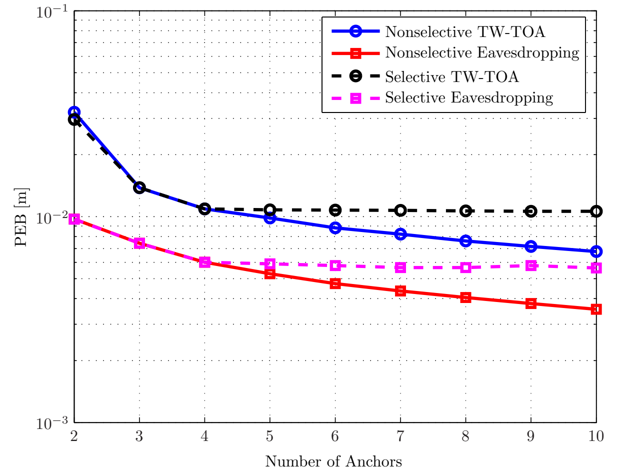

Figure 2. PEB for clique network with 10 agents and increasing number of anchors.

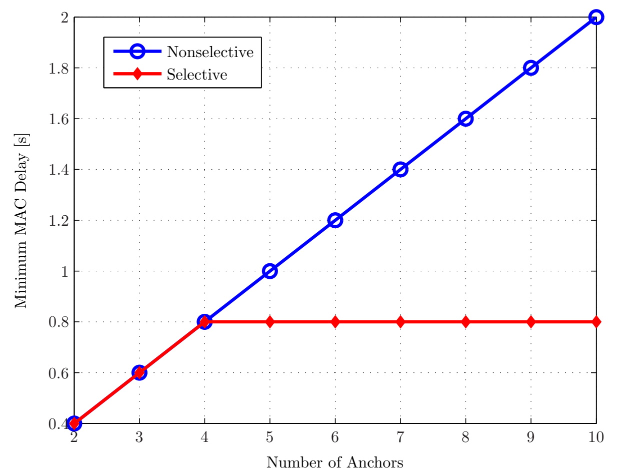

Figure 3. MAC delay for clique network with 10 agents and increasing number of anchors.

B. Impact of Number of Anchors

Figs. 2 and 3 illustrate for a clique network the impact on the localization accuracy and MAC delay when the number of anchors is increased from 2 to 10. Given that the upper and lower bounds for the MAC delay are the same for a clique network, Fig. 3 only depicts the lower bounds. For scenario (i), the PEB decreases as anchors are added since more agent-to-anchor information is gathered by each agent. However, this induces a MAC delay, linearly increasing in M. For scenario (ii), we observe an improvement in the positioning accuracy because of eavesdropping, without any extra MAC delay. When using selective ranging (scenarios (iii)–(iv)), we see that the PEB flattens out to around 1 cm, as does the MAC delay, beyond $M = 4$.

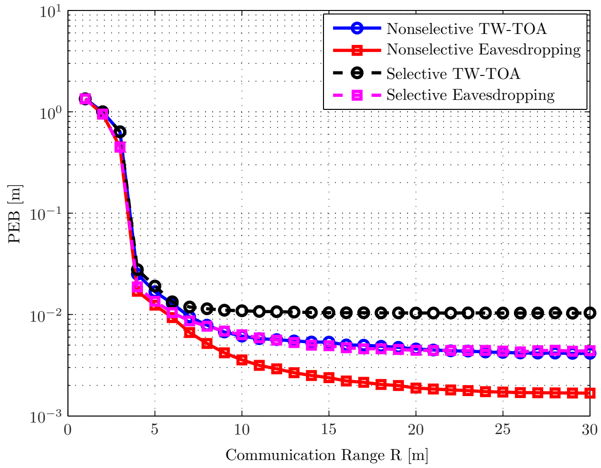

Figure 4. PEB for partially connected network and increasing R.

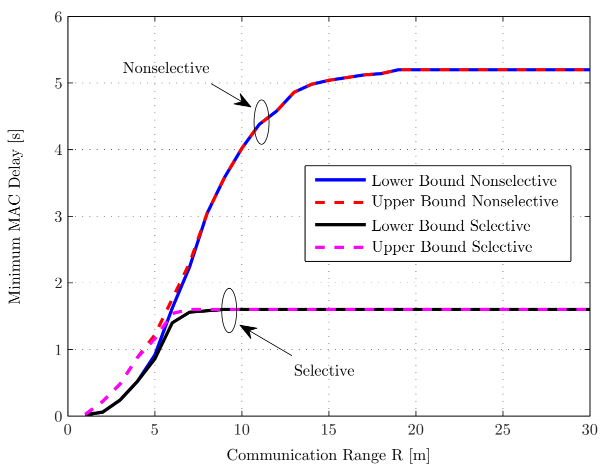

Figure 5. MAC delay for partially connected network and increasing R.

C. Impact of Communication Range

Figs. 4 and 5 depict the impact of incrementing the communication range R from 1 m to 30 m within a network consisting of 20 agents and 13 anchors. As before, the PEB reduces with increasing R. The MAC delay grows fast with increasing R, reaching up to $N \times M \times 20\,\text{ms} \approx 5$ seconds in the scenarios without selective ranging. This clearly shows that increasing R for a marginal gain in terms of accuracy can lead to large delays. Selective ranging enables accurate positioning at a PEB of around 1 cm with reasonable delays (below $N \times 4 \times 20\,\text{ms} \approx 1.6\,\text{s}$).

VI. Conclusions

We have studied the connection between UWB positioning performance and MAC delay, based on parameters from real UWB radios. By deriving lower bounds on the positioning accuracy and the MAC delay for arbitrary networks, we find that the traditional means to improve accuracy (increased number of anchors, increased communication range) comes at a significant cost in terms of delay. This is detrimental for mobile networks, as it reduces the update rate. For a given target accuracy, the delay can be reduced by simple techniques such as selective ranging and eavesdropping.

Our study did not consider the delay T_{comp} related to performing the correction operation. In the case of eavesdropping this time may be non-negligible. Our future work will evaluate this additional delay and also consider cooperative networks with inter-agent ranging.

Appendix

Due to the independence of the TW-TOA measurements, the covariance matrix $\mathbf{\Sigma}$ is a block diagonal matrix, with the block corresponding to $\mathbf{z}_{ij}$ given by

$$\mathbf{C}_{ij} \quad = \quad \mathbb{E}\left\{(\mathbf{z}_{ij} - \boldsymbol{\mu}_{ij})(\mathbf{z}_{ij} - \boldsymbol{\mu}_{ij})^{\mathrm{T}}\right\},$$

with

$$\begin{aligned}
\mathbb{E}\left\{(z_{ij} - \mu_{ij})^2\right\} &= \frac{\sigma_{ij}^2 + \sigma_{ji}^2}{4} \\
\mathbb{E}\left\{(z_{ij} - \mu_{ij})(z_{ij}^k - \mu_{ij}^k)\right\} &= \frac{\sigma_{ij}^2}{2} \\
\mathbb{E}\left\{(z_{ij}^l - \mu_{ij}^l)(z_{ij}^k - \mu_{ij}^k)\right\} &= \begin{cases} \sigma_{ij}^2 + \sigma_{jk}^2 + \sigma_{ik}^2 & k = l \\ \sigma_{ij}^2 & k \neq l. \end{cases}
\end{aligned}$$

Note that when there are only TW-TOA measurements, $\mathbf{C}_{ij}$ reverts to the scalar $(\sigma_{ij}^2 + \sigma_{ji}^2)/4$.

References

[1] A. F. Molisch, P. Orlik, Z. Sahinoglu, and J. Zhang, "UWB-based sensor networks and the IEEE 802.15.4a standard - a tutorial," *International Conference on Communication and Networking in China*, 2006.

[2] Y. Shen and M. Z. Win, "Fundamental limits of wideband localization - part I: A general framework," *IEEE Transactions on Information Theory*, vol. 56, pp. 4956–4980, 2010.

[3] H. Wymeersch, J. Lien, and M. Z. Win, "Cooperative localization in wireless networks," *Proceedings of the IEEE*, vol. 97, pp. 427–450, 2009.

[4] "P400 data sheet," Time Domain Corp., Huntsville, AL, USA.

[5] I. Bucaille, A. Tonnere, L. Ouvry, and B. Denis, "MAC layer design for UWB LDR systems: PULSERS proposal," *4th Workshop on Positioning, Navigation and Communication*, 2007.

[6] D. Macagnano, G. Destino, F. Esposito, and G. Abreu, "MAC performances for localization and tracking in wireless sensor networks," *4th Workshop on Positioning, Navigation and Communication*, 2007.

[7] B. Denis, M. Maman, and L. Ouvry, "On the scheduling of ranging and distributed positioning updates in cooperative IR-UWB networks," *International Conference on UWB*, pp. 370–375, 2009.

[8] F. Sottile, A. Vesco, R. Scopigno, and M. Spirito, "MAC layer impact on the performance of real-time cooperative positioning," in *Wireless Communications and Networking Conference (WCNC)*, 2012, pp. 1858–1863.

[9] M. R. Gholami, S. Gezici, and E. G. Ström, "Improved position estimation using hybrid TW-TOA and TDOA in cooperative networks," *IEEE Transactions on Signal Processing*, vol. 60, pp. 3770–3785, 2012.

[10] U. Orguner and F. Gustafsson, "Target tracking with particle filters under signal propagation delays," *IEEE Transactions on Signal Processing*, vol. 59, pp. 2485–2495, 2011.

[11] C. Pedersen, T. Pedersen, and B. H. Fleury, "Exploiting network topology information to mitigate ambiguities in VMP localization," *4th IEEE International Workshop on Computational Advances in Multi-Sensor Adaptive Processing*, pp. 57–60, 2011.

[12] N. Abramson, "The throughput of packet broadcasting channels," *IEEE Transactions on Communications*, vol. com-25, no.1, pp. 117–128, 1977.

[13] R. Faudree, A. Gyárfas, R. H. Schelp, and Z. Tuza, "Induced matchings in bipartite graphs," *Discrete Math.*, vol. 78, no. 1-2, pp. 83–87, Nov. 1989.